Total X-ray Scattering (TXS) Plugin

1. Introduction

The local structure of materials is closely related to their functional properties, a subject that has been extensively studied for cathode materials,[1, 2] solid electrolytes[3–5] and anode materials[6, 7] for Li-ion batteries, ferroelectric materials ($BaTiO_3$),[8–10] and so forth. Pair distribution function (PDF) analysis is widely used to evaluate local structure in materials. The PDF $G(r)$ is directly obtained from the Fourier transform of the structure factor $S(Q)$, which is calculated from an experimental total scattering pattern. Many PDF analysis results focus on whether or not the calculated value $G_{calc}(r)$ reproduces the observed value $G_{obs}(r)$ using the unit-cell of crystalline structures and many other parameters (e.g., broadening factor, damping factor, etc.). PDF is a one-dimensional function depending only on distance r, and it enables the evaluation of interatomic distances and coordination numbers. However, it is difficult to perform precise analysis of local atomic arrangements (e.g., the displacement histogram of each element, the angular histogram and etc.). Total scattering analysis is often used not only for $G(r)$ but also for $S(Q)$ to analyze such three-dimensional local structure. Figure 1 shows the relationship between total scattering analysis and PDF analysis. It indicates PDF analysis is a part of the total scattering analysis.

Recently, there has been an increasing demand to perform local structural analysis using a laboratory instrument that can measure the total scattering profile to a wide Q range. We have already reported that SmartLab equipped with an Ag rotating anode tube and a Si pixel detector for high-energy X-rays can perform the total scattering measurement with extremely low background.[11] The $S(Q)$ for SiO_2 glass measured by SmartLab has the same quality as that obtained from a synchrotron facility, as shown in Fig. 2.[11] Furthermore, we have released the RMC option, an improved RMC method originally proposed by R. L. Mcgreevy and L. Puzai,[12] in the total scattering analysis plugin of SmartLab Studio II (SLSII). The RMC option can easily evaluate the local structure in a crystalline material. Moreover, we changed the plugin name from "*PDF plugin*" to "*Total X-ray Scattering (TXS) analysis plugin*" based on the concept that *PDF analysis is a part of total scattering analysis*.

In this paper, we introduce the basic functions and features of the TXS analysis plugin using actual analysis data.

2. Features of the TXS Analysis Plugin

The TXS analysis plugin is the successor of the PDF calculation from the legacy PDF plugin and adds a local structural modeling function using the RMC method. The TXS analysis plugin has the following three features: ①PDF calculation from the total scattering profile, ②a local structural modeling function by RMC method, ③statistics calculated from the revised local structural model.

2.1 $G(r)$ calculation from total scattering profile

The basic option of the TXS analysis plugin can

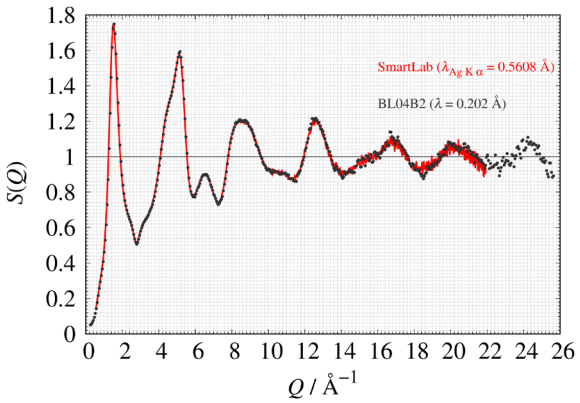

Fig. 2. The comparison of SiO_2 glass structure factor $S(Q)$. Red solid line: SmartLab, black filled circle: BL04B2 in SPring-8.

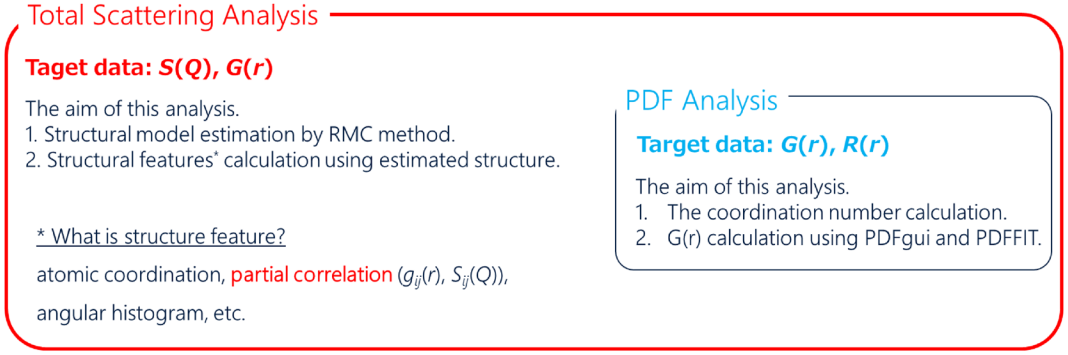

Fig. 1. The relationship between total scattering analysis and PDF analysis.

calculate the structure factor $S(Q)$ and PDF $G(r)$ from total scattering data as shown in Fig. 3. Rigaku's unique data correction method, ripple removal correction, which is effective for eliminating unphysical oscillations that appear before the first peak position, is implemented in the TXS analysis plugin. Furthermore, by improving this correction method, the number density of a specimen can be estimated from the total scattering profile.[13), (14)] The method to determine the number density will be implemented in SLSII ver. 5.0.

2.2 RMC option

As described above, the RMC option in SLSII can estimate a local structural model by the RMC method. Here are four features of the RMC option:

1. It is available on the same flow bar from the analysis of experimental profiles to RMC modeling, as shown in Fig. 4.
2. It is easy to switch the target function for RMC calculations between $S(Q)$ and $G(r)$ in either direction, as shown in Fig. 5.

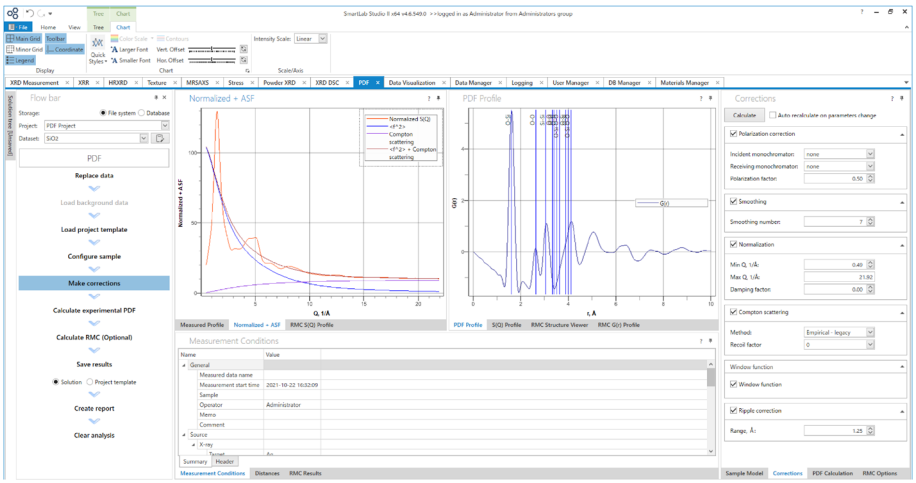

Fig. 3. The main window for calculating PDF profile from experimental data.

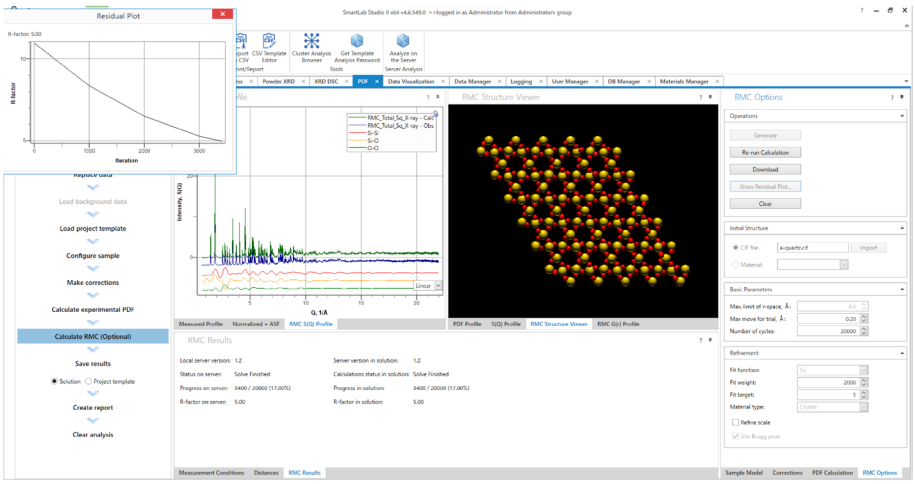

Fig. 4. The main window performing the RMC calculation

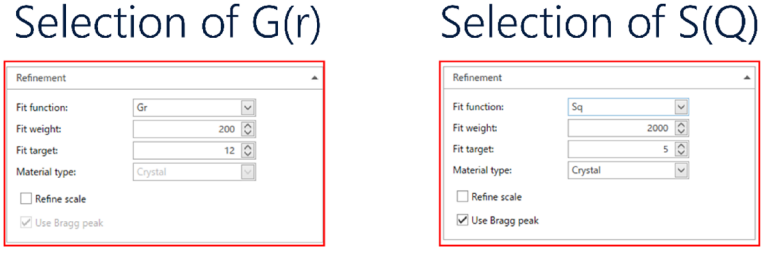

Fig. 5. The window used to set the target function for the RMC calculation. Left: structural refinement to $G(r)$, right: structural refinement to $S(Q)$.

3. Even if there is a defect in the crystalline structure (e.g., a site occupancy is smaller than one), the RMC option can easily generate an initial structural model and perform local structural modeling.
4. The GUI supports a wide range of users, from beginner to specialist, as shown in Fig. 6.

The TXS analysis plugin can perform total scattering analysis from PDF calculation to RMC modeling with a single flow bar. It is not necessary to switch from the PDF calculation to another program for structural modeling. Moreover, the RMC option requires fewer parameters for RMC modeling than other RMC software (e.g., RMCProfile, RMC++, etc.). Therefore, all users can easily evaluate the local structure features in a specimen. For crystalline materials, the RMC option uses Rigaku's original algorithm.[15]

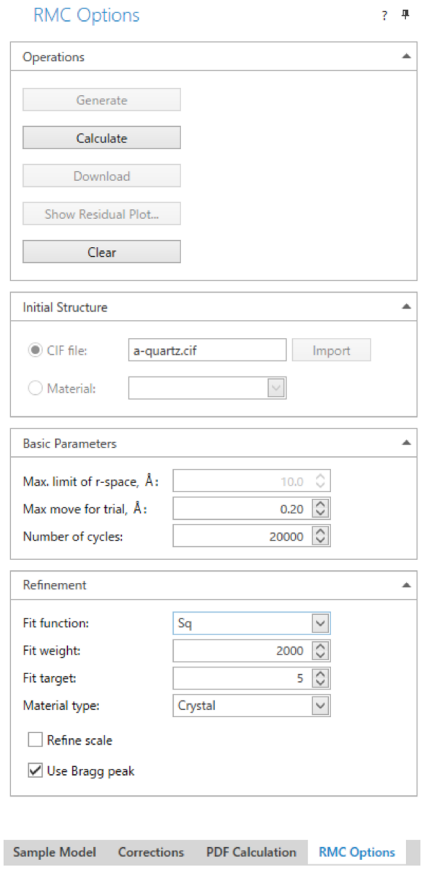

Fig. 6. The window for setting the conditions for the RMC calculation.

The TXS analysis plugin supports not only structural modeling by the RMC method but also an analyzing tool to calculate statics after RMC modeling. In SLSII ver. 5.0, the RMC option can calculate five types of statistics from the structural model: I. partial correlation (i.e., partial structure factor and partial pair distribution function), II. collapsed model, III. the gravimetric center calculated from the collapsed model, IV. the volume data of the density distribution of each site, and V. the displacement histogram of each element using II and III.

3. Application

In this section, we introduce local structural features of α-quartz estimated by RMC method. Figure 7 shows the $S(Q)$ comparison and the estimated structural model displayed in the *VESTA*[16] program. We have constructed an α-quartz structural model consistent with the observed $S_{obs}(Q)$ by RMC method. The R-factor, which indicates the degree of agreement between the observed and calculated values, is R_p = 3.0%. The summation of Si–O and O–O weighted partial correlations is in agreement with the fringe in $S_{obs}(Q)$ arising at the high-Q region, indicating that the SiO_4 tetrahedral structure remains in the estimated α-quartz structure (Fig. 8). Furthermore, the peaks in the $G_{obs}(r)$ can be evaluated using the weighted partial pair distribution function shown in Fig. 9. Figure 11 shows the center of gravity and the corresponding voxel data of density distribution of each atom, calculated from the collapsed model in Fig. 10. Table 1 shows the average displacement and the corresponding standard deviation of each atom. Si atoms show a spherical density distribution in Fig. 11. On the other hand, O atom larger

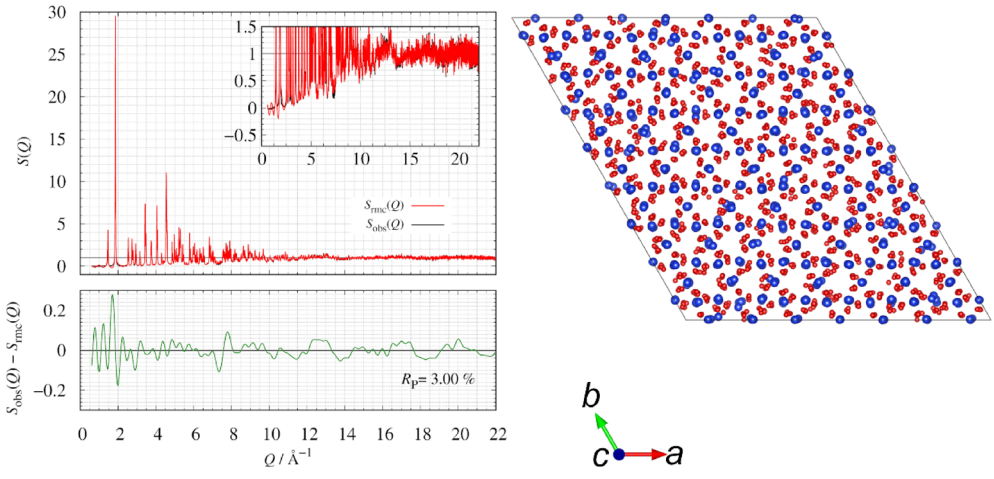

Fig. 7. (Left) Comparison of α-quartz S(Q) between the experimental value (red) and the calculated value (blue). The corresponding residual curve (green). (Right) The estimated structural model of α-quartz.

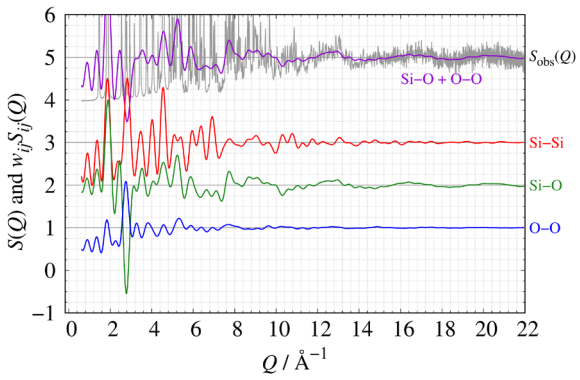

Fig. 8. Comparison of the experimental $S(Q)$ and the weighted partial structure factor $w_{ij}S_{ij}(Q)$.

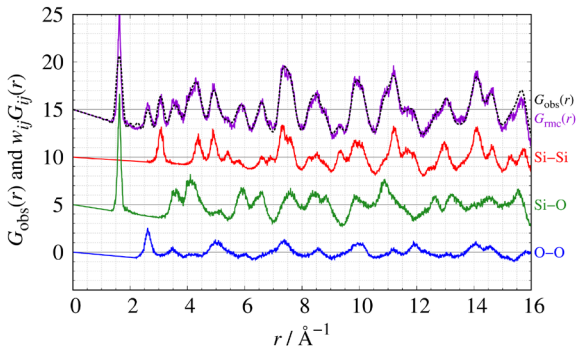

Fig. 9. Comparison of the experimental $G(r)$ and the weighted partial structure factor $w_{ij}G_{ij}(r)$.

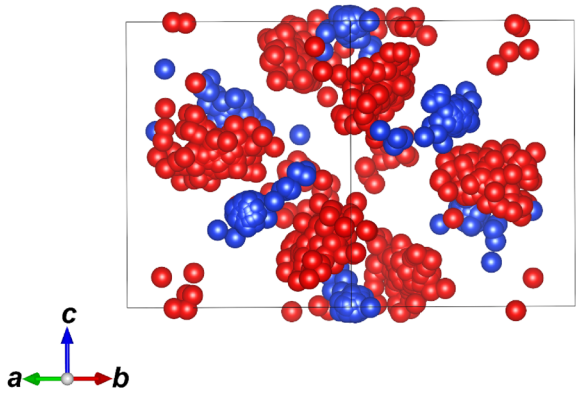

Fig. 10. The collapsed structural model, which is converted from the structural model shown in Fig. 7 into unit-cell dimensions. Red: Oxygen atom, blue: silicon atom. Each atom is shown as a sphere whose radius is 0.5 Å.

displacement than the Si atoms and exhibit an ellipsoidal density distribution in Fig. 11.

4. Summary

We have introduced the TXS analysis plugin. Applications beyond those presented here, have been reported in articles.[13, 15, 17)]

In the near future, we will release these new functions in the TXS analysis plugin: 1. estimated number density

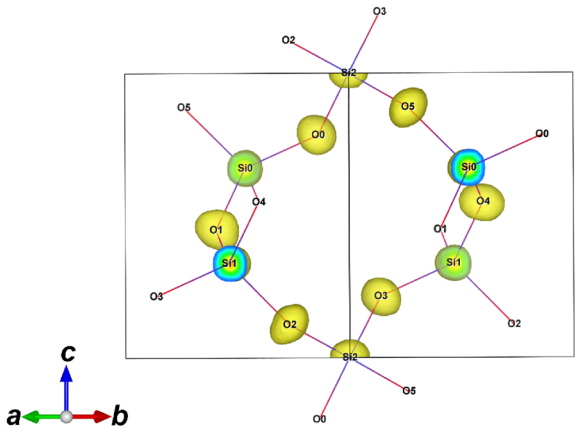

Fig. 11. The position of the center of gravity and the density distribution of each site calculated from the estimated structural model by RMC modeling. The Si–O bond length is presented less than 2 Å. the present label of each site

Table 1. The average displacement momentum Δr and the corresponding standard deviation σ calculated from the collapsed model in Fig. 2 and the center of gravity in Fig. 4. The site name is the same as each site in Fig. 4.

The site name	The average displacement Δr (Å)	The standard deviation σ(Å)
Si0	0.061	0.130
Si1	0.053	0.101
Si2	0.042	0.092
O0	0.108	0.204
O1	0.123	0.184
O2	0.104	0.145
O3	0.111	0.157
O4	0.114	0.179
O5	0.114	0.171

method calculated from $S(Q)$, 2. displacement histogram of each atom and angular histogram calculated from the revised structural model by RMC modeling.

Reference

(1) K. Ishidzu, Y. Oka, and T. Nakamura: *Solid State Ionics,* **288** (2016) 176–179. https://doi.org/10.1016/j.ssi.2016.01.009.

(2) T. Ohnuma and T. Kobayashi: *RSC Adv.*, **9** (2019) 35655–35661. https://doi.org/10.1039/C9RA03606G.

(3) J.G. Smith, D.J. Siegel, *Nat. Commun.*, **11** (2020) 1483 (11pp). https://doi.org/10.1038/s41467-020-15245-5.

(4) T. Scholz, C. Schneider, M. W. Terban, Z. Deng, R. Eger, M. Etter, R. E. Dinnebier, P. Canepa, and B. V. Lotsch: *ACS Energy Lett.*, **7** (2022) 1403–1411. https://doi.org/10.1021/acsenergylett.1c02815.

(5) H. Yamada, K. Ohara, S. Hiroi, A. Sakuda, K. Ikeda, T. Ohkubo, K. Nakada, H. Tsukasaki, H. Nakajima, L. Temleitner, L. Pusztai, S. Ariga, A. Matsuo, J. Ding, T. Nakano, T. Kimura, R. Kobayashi, T. Usuki, S. Tahara, K. Amezawa, Y. Tateyama, S. Mori, A. Hayashi, *Energy & Environ Materials*. (2023) e12612 (10pp). https://doi.org/10.1002/eem2.12612.

(6) I. Umegaki, S. Kawauchi, H. Sawada, H. Nozaki, Y. Higuchi, K. Miwa, Y. Kondo, M. Månsson, M. Telling, F. C. Coomer, S. P. Cottrell, T. Sasaki, T. Kobayashi, and J. Sugiyama: *Phys*. *Chem*. *Chem*. *Phys*. **19** (2017) 19058–19066. https://doi.org/10.1039/C7CP02047C.
(7) J. Asenbauer, T. Eisenmann, M. Kuenzel, A. Kazzazi, Z. Chen, and D. Bresser: *Sustain. Energ. Fuel*., **4** (2020) 5387–5416. https://doi.org/10.1039/D0SE00175A.
(8) T.-C. Huang, M.-T. Wang, H.-S. Sheu, and W.-F. Hsieh: *J. Phys*.: *Condens*. *Matter*., **19** (2007) 476212 (12 pp). https://doi.org/10.1088/0953-8984/19/47/476212.
(9) T. Hoshina: *J. Ceram*. *Soc*. *Japan*, **121** (2013) 156–161. https://doi.org/10.2109/jcersj2.121.156.
(10) Y. Yoneda, S. Kim, S. Mori, and S. Wada: *Jpn*. *J*. *Appl*. *Phys*., **61** (2022) SN1022 (10pp). https://doi.org/10.35848/1347–4065/ac835d.
(11) M. Yoshimoto, and Y. Shiramata: *Rigaku Journal,* **36,** No. 1 (2020) 10–18.
(12) R. L. McGreevy, and L. Pusztai: *Mol*. *Simul*., **1** (1988) 359–367. https://doi.org/10.1080/08927028808080958.
(13) M. Yoshimoto, and K. Omote: *J*. *Phys*. *Soc*. *Jpn*., **91** (2022) 104602 (7pp). https://doi.org/10.7566/JPSJ.91.104602.
(14) M. Yoshimoto: *Rigaku Journal,* **39**, No. 1 (2023) 15–23.
(15) M. Yoshimoto, and K. Omote: *Appl*. *Phys*. *Exp*., **16** (2023) 015005 (4pp). https://doi.org/10.35848/1882-0786/acb2b0.
(16) K. Momma, and F. Izumi: *J*. *Appl*. *Crystallogr*., **44** (2011) 1272–1276. https://doi.org/10.1107/S0021889811038970.
(17) M. Yoshimoto, T. Kimura, A. Sakuda, C. Hotehama, Y. Shiramata, A. Hayashi, and K. Omote: *Solid State Ionics*, **401** (2023) 116361 (8 pp). https://doi.org/10.1016/j.ssi.2023.116361.